

Synthesis and Study of Temperature Effect on the Spectroscopic Properties of The Nickel Ferrites by Glycine-Nitrate Auto-Combustion

We'am Sami

Department of Physics, College of Education, University of Al-Qadisiyah, Qadisiyah, Iraq.

*Corresponding author E-mail: weam.sami@qu.edu.iq

Doi:10.29072/basjs.20220108

ARTICLE INFO

ABSTRACT

Keywords

Ferrite;
Photoluminescence;
nanoparticles;
auto-combustion;
spectroscopic
properties

The spinel Ni-ferrite with different synthesizing temperature was synthesized by the glycine-nitrate auto-combustion process. X-ray diffraction, field emission-scanning electron microscopy, Fourier transform-infrared spectroscopy and Photoluminescence analysis were used to characterize structural, morphological and optical properties of the as-synthesized samples. The XRD results revealed that the as-synthesized samples possess a cubic spinel structure and the lattice constant decreases from 8.3435 Å to 8.3321Å when the synthesis temperature rises from 50°C to 100°C. Further, Increasing the synthesis temperature led to increase the crystallite size from 25 nm to 32 nm. FE-SEM images show that the nanoparticles have agglomerated. FTIR spectra supported the formation of the Ni-ferrite structure and show that the absorption band of a particular bond is shifted to the higher frequency with a rise in temperature. Photoluminescence (PL) spectrum consists of emission peaks at 350 nm (3.54 eV), 680 nm (1.82 eV), 770 nm (1.61 eV), and 820 nm (1.51 eV). The PL peaks were shifted to shorter wavelengths with an increase in the emission intensity when increasing the temperature of synthesis.

Received 12 Mar 2022; Received in revised form 9 Apr 2022; Accepted 25 Apr 2022, Published 30 Apr 2022



1. Introduction

Nanoparticles retain a variety of physical physiognomies and chemical characteristics different from the corresponding bulk stable state properties due to the quantum size effect, dimensions, surface influence, or quantum tunnelling impact. Metallic nanoparticles have previously been thoroughly investigated due to their theoretical and technical significance for a wide range of applications[1]. Ferrites are complex oxides derived from the magnetite by replacing a divalent iron atom with another transition metal atom . Ferrites can be divided into three groups based on their crystal structures: spinel ferrites, garnet ferrites and hexagonal ferrites [2]. Synthesis and characterization of spinel ferrites at nanoscale have drawn much attention because nanoparticles with large surface to volume ratios have enhanced magnetic, electrical, optical properties which in turn found potential applications[3] such as magnetic fluid, high density data storage, catalyst, gas sensors, water purification, etc.[4].The nano NiFe_2O_4 with a spinel structure is one of the promising candidates which has been used in different fields such as photocatalytic activity [5], biomedical efficiency[6] and cancer hyperthermia[7].The nano NiFe_2O_4 with a spinel structure has the general formula AB_2O_4 [8]. In this structure, O specifies the oxygen anion site A and B shows tetrahedral and octahedral cation sites. The nickel ions (Ni^{+2}) are occupied B sites and iron ions (Fe^{3+}) are equally dispersed between A and B sites [9] as shown in Fig. 1.

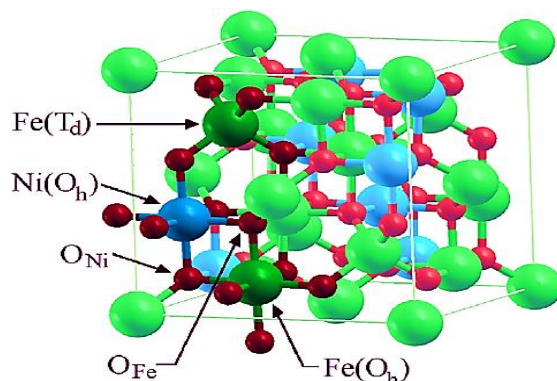


Figure1: Schematic representation of NiFe_2O_4 structure [10].

In recent years, NiFe_2O_4 nanoparticles has been prepared by different process like sonochemical method [11], hydrothermal method [9], conventional sol-gel [12] self-ignited auto-



combustion method [13]. Accordingly, present investigation aimed to prepared nickel ferrite nanopowder with glycine-nitrate auto-combustion process, using different preparation temperatures, and to examine their spectroscopy properties.

2. Materials and Method

Nitrate salts of nickel ($\text{Ni}(\text{NO}_3)_2 \cdot 6\text{H}_2\text{O}$) and ferric ($\text{Fe}(\text{NO}_3)_3 \cdot 9\text{H}_2\text{O}$) were used. The following steps were taken to synthesis Ni-ferrite by glycine-nitrate auto-combustion process. (i) The required amount of high purity $\text{Fe}(\text{NO}_3)_3 \cdot 9\text{H}_2\text{O}$ and $\text{Ni}(\text{NO}_3)_2 \cdot 6\text{H}_2\text{O}$ from HIMEDIA Co., India were used as starting materials with a molar ratio 1:2 of Ni(II)/Fe(III) and dissolved in a suitable quantity of de-ionized water. (ii) The solutions were mixed thoroughly using a magnetic stirrer for 20 minutes at an auto-combustion temperature of $(50)^\circ\text{C}$. (iii) The required amount of glycine was added into the nitrate solution under stirring without heat exchange. After vaporization of the entire amount of water, the self-sustained combustion reaction was initiated in the system. (iv) Powder product was washed via ethanol and distilled water for (4) times, dried at (80°C) for 2 hours. (v) Mortar was used to grind the resulting powder for (4min.) in order to result in fine NiFe_2O_4 ferrites ash. (vi) The same steps from (i-v) were followed to synthesize the Ni-ferrite at preparation temperature at 75°C and 100°C . The X-ray diffraction analyses were obtained from the (Shimadzu XRD 6000, Japan) at the University of Baghdad, Iraq. Morphology and elemental analyses were examined with Field Emission- Scanning Electron Microscope (TE-SCAN Mira3, France) at the University of Mashhad, Iran.

To determine the chemical structure of the synthesized Ni-ferrite powders the FTIR spectrum was taken using an (Shimadzu-8400S spectrometer) at the range of $(4000 - 450 \text{ cm}^{-1})$ (as pellets in KBr) at Chemical Analysis Center (CAC), Iraq. The photoluminescence study of the Ni-ferrite nanoparticles recorded with an excitation wavelength of 385 nm at the University of Mashhad, Iran

3. Results and Discussion

3.1 Phase Formation and Structural Analysis

The XRD pattern for three different NiFe_2O_4 ferrite products was exhibited in Fig. 2. The diffraction peaks (220), (311), (400), (422), (511) and (440) appear in all the samples. The presence of these peaks of diffraction indicates that the existing system has a cubic spinel structure according to (JCPDS card No. (00-054-0964)) of the NiFe_2O_4 . In nickel ferrite prepared at the temperature of the synthesis (50°C) , the impurity phase Fe_2O_3 ($2\theta = 33.7^\circ$ and 41.5°) was



observed. This impurity phase decreases with a rise in temperature of the synthesis as shown in Fig.2. The rise in the temperature of the synthesis contributes to an increase in grain size, resulting in narrow and sharp peaks indicating to enhance the crystallinity of prepared samples; however the peak of the XRD spectra for the other spinel Ni-ferrite powder samples synthesized at temperatures of 100°C are sharper compared to previous peaks.

The crystallite size (D) of synthesized NiFe₂O₄ samples was calculated through Debye Scherrer formula by measuring the FWHM of the highest peak (311) plane, while the lattice constant (a) was estimated through eq.2 below [4,14]. All these parameters were calculated for the samples are listed in Table1.

$$D = \frac{0.9\lambda}{\beta \cos\theta} \quad 1$$

$$a = d_{hkl} \sqrt{h^2 + k^2 + l^2} \quad 2$$

Where λ represents the XRD wavelength that used (1.1548 Å), β - is represent Full Width Half Maximum of plane (311) , θ - is represent the Bragg's angle, d- is represent interplanar spacing values and (hkl) the Miller indices.

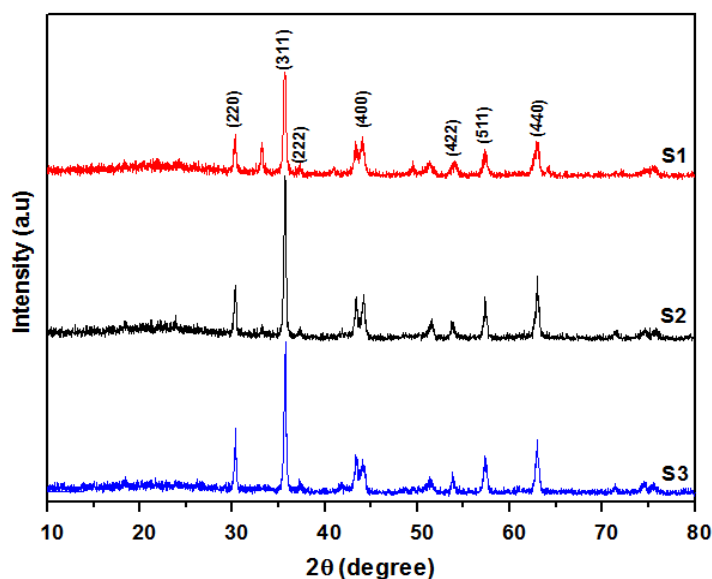


Figure 2: XRD patterns of spinel NiFe₂O₄ powders at different synthesizing temperatures by glycine-nitrate auto-combustion process.(S1): T: 50°C,(S2): T: 75°C and (S3): T: 100°C.

Table 1: Crystallite size and lattice constant of NiFe₂O₄ powders at different synthesizing temperatures

as-synthesized powdered samples	T (°C)	2θ (deg.)	Lattice spacing, d (Å)	Lattice constant a (°Å)	Crystallite size D (nm)
S1	50	35.66	2.51568	8.3435	25
S2	75	35.69	2.51357	8.3365	30
S3	100	35.71	2.51223	8.3321	32

From Table 1, it is clear that the crystallite size of the spinel phase increased from 25nm to 32nm. The reason may be due to the enhancement of the coalescence process, which takes place at high synthesizing temperatures with respect to time, in which the grain size of the final products increases. Based on the literature, crystallite size and lattice constant are directly related. Decreasing in crystallite size led to an increase or decrease in the lattice constant [15]. In the present work, lattice constant decreases with the rise of temperature and increasing in the crystallite size. A similar variation was observed by H. Moradmard et al. [16].

3.2 Surface Morphology

The morphology characterization of spinel NiFe₂O₄ powders were determined by FE-SEM analysis. The FE-SEM images of the samples at the lowest and highest temperature are shown in Fig.3a and the EDS spectrum is given in Fig.3b. From FE-SEM images, it can be observed that the nanoparticles have agglomerated. Agglomerate and grow into larger assemblies a cure when the nanoparticles have a large surface area-to-volume ratio and very high surface energy. In order to reduce the total surface energy, the particles in the nanoscale tend to agglomerate. Another reason for agglomeration may be the interaction between the magnetic nanoparticles that is agrees with D. Guragain etal. [8]. The effects of the escaped gases during the combustion phase could be the voids in the powdered samples. EDX analysis for Ni-ferrite at lowest and highest temperature indicates that the basic compositions of ferrites are Ni, Fe and O. Au peak impurity in samples due to the ferrite samples were coated with gold for the avoidance of charging effect.



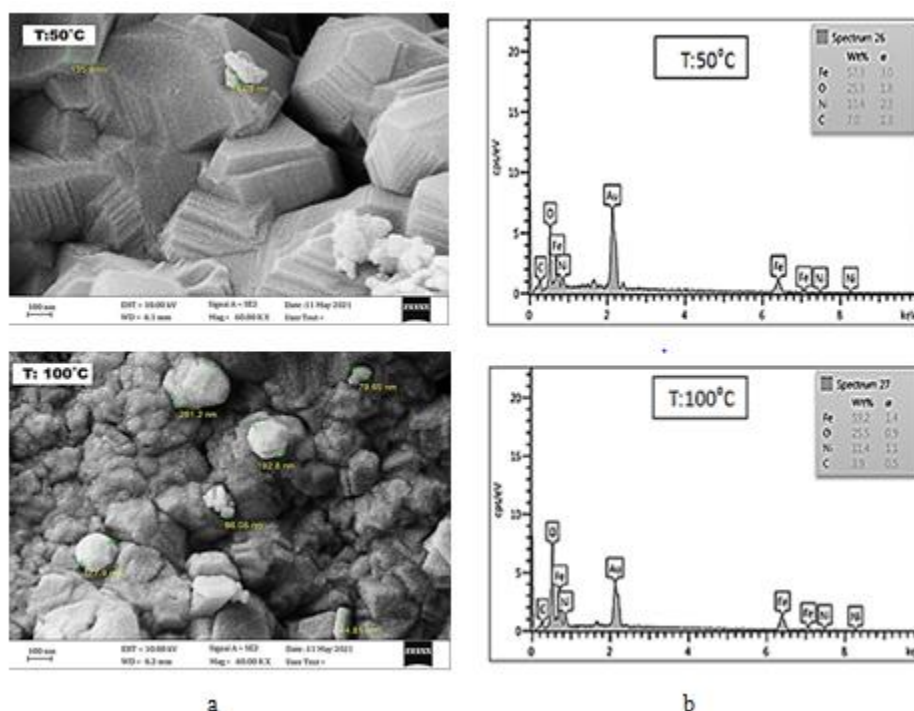


Figure 3: (a) FE-SEM images and (b) EDS analysis of the spinel Ni- Fe_2O_4 ferrite samples

3.3 Fourier Transforms -Infrared Spectroscopy Analysis

To determine the chemical structure of the synthesized Ni-ferrite powders the FTIR spectrum was taken at the range of $(4000 - 450 \text{ cm}^{-1})$ (as pellets in KBr) and shown in Fig. 4. The main two vibrational bands were observed in FT-IR spectra for S1, one is higher vibrational frequency (ν_{Tet}) in the range of 554.76 cm^{-1} and the other one is the lower vibrational frequency (ν_{Oct}) in the range of 464.12 cm^{-1} , are the characteristic bands of cubic spinel structure. The higher vibrational frequency ν_{Tet} is assigned to Fe^{3+} - O^{2-} stretching vibrations at the tetrahedral site (A) and the lower vibrational frequency ν_{Oct} variation at the octahedral site (B). A similar variation was observed in Ref. [17]. Compared between the three samples in Figure 4, it is clear that no lower vibrational frequency ν_{Oct} variation in octahedral site (B) appeared in the spectrum at highest temperatures (75 and 100) $^\circ\text{C}$. The reason is the inability to read the value less than 500 cm^{-1} for FT-IR device. The peak at $\sim 2333 \text{ cm}^{-1}$ was ascribed to stretching vibration of the O-H group present in the nanoferrites. The special absorption peak at 2920.89 cm^{-1} corresponds to O-H group of fuel [13]. The hydroxyl group can be assigned to the wide band around 3778.94 cm^{-1} . Similar variation was observed in Ref. [18] for other spinel ferrite. Depending on the method suggested by Waldron [19] the force constant (K_{Tet} and K_{Oct}) of the tetrahedral and octahedral vibrational frequencies (ν_{Tet} and ν_{Oct}) are listed in Table 2. It is clear that the



tetrahedral vibrational frequencies is shifted towards the higher frequencies with a rise in temperature, which are ascribed to increase in force constants and contraction of $\text{Fe}^{3+} - \text{O}^{2-}$ bond lengths at A site

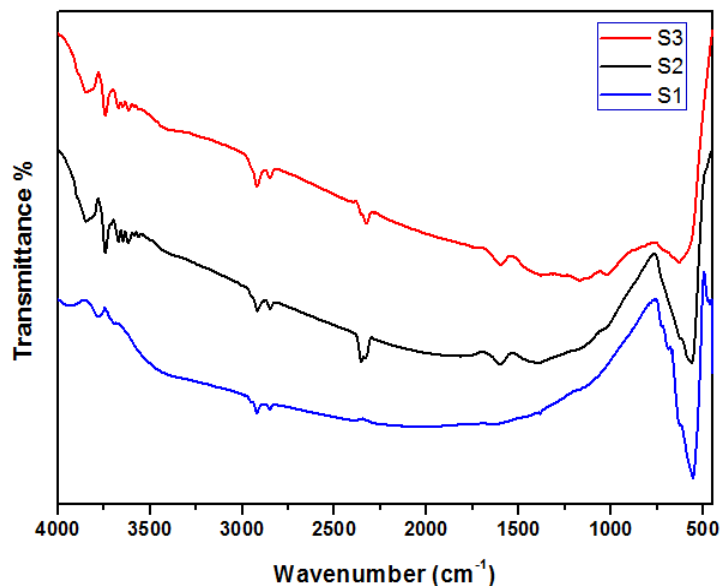


Figure 4: FT-IR spectrum for three as-synthesized powdered Ni-ferrite by glycine-nitrate auto-combustion process.(S1): T: 50°C,(S2): T: 75°C, and (S3): T: 100°C.

Table 2: The tetrahedral and octahedral vibrational frequencies as well as force constants of Ni-ferrites at different synthesizing temperatures.

Sample	T (°C)	XRD D(nm)	ν_{Tet} (cm^{-1})	ν_{Oct} (cm^{-1})	K_{Tet} (10^2 N/m)	K_{Oct} (10^2 N/m)
S1	50	24.64	554.76	464.12	2.23	1.56
S2	75	30	562.15	-	2.29	-
S3	100	32.09	629.26	-	2.88	-

3.4 Photoluminescence analysis

The photoluminescence study of the Ni-ferrite nanoparticles was recorded at room temperature with an excitation wavelength of 385 nm and depicted in Fig. 5. The spectra were found in the visible region. The spectrum consists of emission peaks at 350 nm (3.54 eV), 680 nm (1.82 eV), 770 nm (1.61 eV), and 820 nm (1.51 eV). Peaks were shifted to shorter



wavelengths with an increase in the emission intensity as temperature rising. The Photoluminescence around 3.54 eV is mainly because of the quantum confinement because the peak value approximately agrees with the band gap of ferrite nanomaterials.

The influence of the surface oxide is also essential if there is a difference in the energies, which is associated with the Stokes shift between the absorption surface defects or surface oxide. Similar observations were reported for other ferrites in Ref. [20].

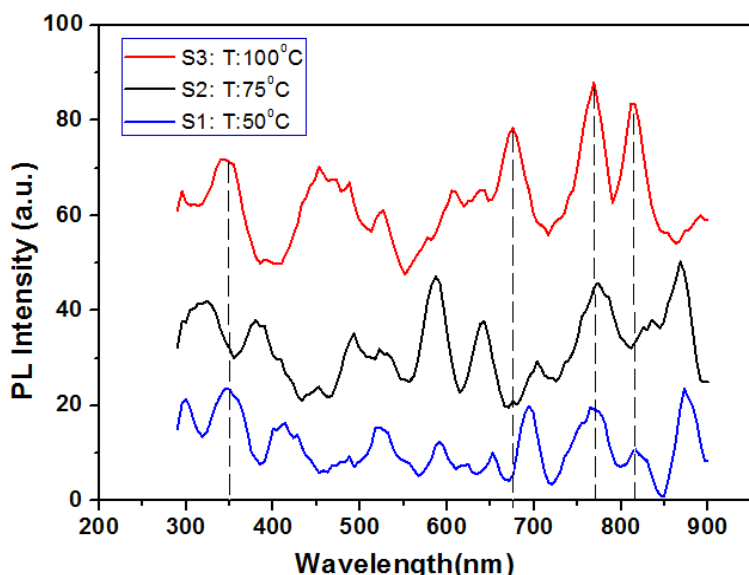


Figure 5: Photoluminescence spectra for three as-synthesized powdered Ni-ferrite by glycine-nitrate auto-combustion process.

4. Conclusions

From the study glycine-nitrate auto-combustion process produces cubic spinel structure of Ni-ferrite nanoparticles with impurity phase Fe_2O_3 at low temperature of 50°C decreases with a rise in temperature of the synthesis. The glycine-nitrate auto-combustion process is suitable for the synthesis of Ni-ferrite nanoparticles with small crystallite size variation (25-32)nm depending on the temperature of the synthesis. Glycine-nitrate auto-combustion process produce Ni-ferrite nanoparticles that have agglomerated. Furthermore, from the photoluminescence study, the emission peaks were shifted to shorter wavelength with an increase in the emission intensity as temperature rising.

Acknowledgments

The author is grateful to the University of Baghdad, Iraq, Chemical Analysis Center(CAC), Iraq, and the University of Mashhad, Iran for providing characterizations facilities for the present work.

References

- [1] S.B. Khan, S. Irfan, S-L. Lee, Influence of Zn⁺² Doping on Ni-Based Nano ferrites; (Ni_{1-x}Zn_xFe₂O₄), J. Nanomater., 9(2019)1-17, <https://doi.org/10.3390/nano9071024>
- [2] W. Sami, Z.S. Sadeq, Role of Glycine-to-Nitrate Ratio in Physical and Magnetic Properties of Zn-Ferrite Powder, Iraqi J. Sci., 63(2022)170-181, <https://doi.org/10.24996/ijs.2022.63.1.18>
- [3] T. Dippong, E.A. Levei, O. Cadar, Recent Advances in Synthesis and Applications of MFe₂O₄ (M=Co, Cu, Mn, Ni, Zn) Nanoparticles, J. Nanomater., 11(2021)1-33, <https://doi.org/10.3390/nano11061560>
- [4] V.A. Bharati, S. R. Patade, S. Bajaj, R. Parlikar, A P Keche, V. V. Sondur, Structural and Magnetic Properties of Nickel Ferrite Nanoparticles Prepared by Solution Combustion Method, J. Phys. Conf. Ser., 1644(2020)1-5, [10.1088/1742-6596/1644/1/012005](https://doi.org/10.1088/1742-6596/1644/1/012005)
- [5] M.P. Tsvetkov, I.R. Ivanova, E.P. Valcheva, J.T. Zaharieva, M.M. Milanova, Photocatalytic Activity of NiFe₂O₄ and Zn_{0.5}Ni_{0.5}Fe₂O₄ Modified by Eu(III) and Tb(III) For Decomposition of Malachite Green , Open Chem. J., 17(2019)1124-1132, <https://doi.org/10.1515/chem-2019-0116>
- [6] H. Q. Alijani, Sh. Pourseyedi, M. Torkzadeh-Mahani, A. Seifalian, M. Khatami, "Bimetallic Nickel-Ferrite Nanorod Particles: Greener Synthesis Using Rosemary and Its Biomedical Efficiency, J. Artif. Cells Nanomed. Biotechnol., 48(2020)42-251, <https://doi.org/10.1080/21691401.2019.1699830>
- [7] D. Saykova, S. Saikova, Y. Mikhlin, M. Panteleeva, R. Ivantsov , E. Belova, Synthesis and Characterization of Core–Shell Magnetic Nanoparticles NiFe₂O₄@Au, J. Met., 10(2020)1-13, <https://doi.org/10.3390/met10081075>
- [8] D. Guragain, B.K. Rai, S. Yoon, T.P. Poudel, S.Ch. Bhandari, S.R. Mishra, Effect of Terbium Ion Substitution in Inverse Spinel Nickel Ferrite: Structural and Magnetic Study, J. Magnetochemistry, 6(2020)1-9, <https://doi.org/10.3390/magnetochemistry6010014>



- [9] J. Hwang, M. Choi and, H-S. Shin, B-K Ju, M.P. Chun, Structural and Magnetic Properties of NiZn Ferrite Nanoparticles Synthesized by a Thermal Decomposition Method, *J. Appl. Sci.*, 10(2020)1-11, <https://doi.org/10.3390/app10186279>
- [10] P.S. da Silva, P.J. Rafael, E.P. Muniz, R.D. Pereira, D.R. Araujo, Applications of Fourier Transform Infrared and X-ray Techniques to Analyze Nickel Ferrite Nanoparticles Produced, *Mater. Sci. Forum*, 727-728(2012)884-887
<https://doi.org/10.4028/www.scientific.net/MSF.727-728.884>
- [11] M.A.S. Amulya, H.P. Nagaswarupa, M.R.A. Kumar, C.R. Ravikumar, S.C. Prashantha, K.B. Kusuma, Sonochemical Synthesis of NiFe₂O₄ Nanoparticles: Characterization and Their Photocatalytic and Electrochemical Applications, *J. Appl. Surf. Sci.*, 1(2020)1-10, <https://doi.org/10.1016/j.apsadv.2020.100023>



- [12] A.A. Khan, M. Javed, A.R. Khan, Y. Iqbal, A. Majeed, S.Z. Hussain, S.K. Durrani, Influence of Preparation Method on Structural, Optical and Magnetic Properties of Nickel Ferrite Nanoparticles, *J. Mater. Sci-Poland.*, 35(2017)58-65, <https://doi.org/10.1515/msp-2017-0006>
- [13] R. Tiwari, M. De, H.S. Tewari, S. K. Ghoshal, Structural and Magnetic Properties of Tailored NiFe₂O₄ Nanostructures Synthesized Using Auto-Combustion Method, *J. Results Phys.*, 16(2020)1-8, <https://doi.org/10.1016/j.rinp.2019.102916>
- [14] W. Sami, Z.S. Sadeq, Synthesis, Characterizations, and Magnetic Properties of Mixed Spinel Mg_{1-x}Zn_xFe₂O₄ Ferrites, *Iraqi J. Sci.*, 63(2022)997-1003, <https://doi.org/10.24996/ij.s.2022.63.3.9>
- [15] L.R. Nivedita, A. Haubert, A.K. Battu, C.V. Ramana, Correlation Between Crystal Structure, Surface/Interface Microstructure, and Electrical Properties of Nanocrystalline Niobium Thin Films, *J. Nanomater.*, 10(2020)1-23, <https://doi.org/10.3390/nano10071287>
- [16] H. Moradmard, S.F. Shayesteh, The Variation of Magnetic Properties of Nickel Ferrite by Annealing, *J. Manuf. Sci. Technol.*, 3(2021)141-145, [10.13189/MST.2015.030411](https://doi.org/10.13189/MST.2015.030411)
- [17] C. Venkataraju, R. Paulsingh, FTIR and EPR Studies of Nickel Substituted Nanostructured Mn Zn Ferrite, *J. Nanosci.*, 2014(2014)1-5, <https://doi.org/10.1155/2014/815385>
- [18] W. Sami, Z.S. Sadeq, Synthesis and Study of Calcination Effect of Zinc Ferrite on the Structure and Morphology of Nanoparticles, *J. Phys. Conf. Ser.*, 1999(2021)1-10, <https://doi.org/10.1088/1742-6596/1999/1/012060>
- [19] M. De, A. Mukherjee, H. S. Tewari, Characterization of Cadmium Substituted Nickel Ferrites Prepared Using Auto-Combustion Technique, *J. Process. Appl. Ceram.*, 9(2015)193-197, [10.2298/PAC1504193D](https://doi.org/10.2298/PAC1504193D)
- [20] R.K. Singh, A. Narayan, K. Prasad, R.S. Yadav, A.C. Pandey, A. K. Singh, L. Verma, R. K. Verma, Thermal, Structural, Magnetic and Photoluminescence Studies on Cobalt Ferrite Nanoparticles Obtained by Citrate Precursor Method, *J Therm Anal Calorim*, 110(2012)573-580, <https://doi.org/10.1007/s10973-012-2728-1>



تؤليف ودراسة تأثير درجة الحرارة على الخواص الطيفية لفرايتات النيكل بواسطة عملية الاحتراق التلقائي

للجلايسين-نترات

وئام سامي

جامعة القادسية، كلية التربية ، قسم الفيزياء

المستخلص

تم تحضير فرايت النيكل نوع السبينيل بدرجات تحضير مختلفة بواسطة عملية الاحتراق التلقائي للجلايسين- نترات. تم استخدام تحليل XRD والمجهر الإلكتروني الماسح للانبعاثات والتحليل الطيفي للأشعة تحت الحمراء لتحويل فورييه وتحليل اللعان الضوئي لتمييز شوائب الطور ، والتشكل والخصائص البصرية لعينات المسحوق المحضرة. أوضحت نتائج XRD أن العينات المُصنَّعة تمتلك بنية إسبنيل مكعبة مع ثابت شبكي ينخفض من (8.3321 Å - 8.3435 Å) عند رفع درجة الحرارة من (50°C-100°C) درجة مئوية. يؤدي رفع درجة الحرارة إلى زيادة حجم البلورات من (25nm - 32nm). تبين صور- FE SEM ان الجسيمات النانوية تمتلك كتل مع وجود فراغات. يدعم طيف FT-IR معلومات تركيب فرايت النيكل حيث تظهر أن نطاق الامتصاص الخاص بالرابطة المعينة يزاح نحو التردد الأعلى مع ارتفاع درجة الحرارة . وجد تحليل اللعان الضوئي في المنطقة المرئية. يتكون الطيف من قمم الانبعاثات عند 350nm (3.54 eV) ، 680nm (1.82 eV) ، 770nm (1.61eV) ، و 820nm (1.51eV). مع رفع درجة الحرارة يتم ازاحة القمم نحو الاطوال الموجية الاقصر بزيادة شدة الانبعاث.

